Int. J. Heat Mass Transfer. Vol. 31, No. 10, pp. 2161–2174, 1988
Printed in Great Britain

0017–9310/88 $3.00 + 0.00

Transient boiling heat transfer characteristics of R113 at large stepwise power generation

KUNITO OKUYAMA

Department of High Temperature Engineering, Japan Atomic Energy Research Institute, Tokai-mura Naka-gun Ibaraki-ken, Japan

and

YOSHIYUKI KOZAWA, AKIRA INOUE and SHIGEBUMI AOKI

Research Laboratory for Nuclear Reactors, Tokyo Institute of Technology, Tokyo, Japan

(*Received* 21 *September* 1987 *and in final form* 1 *April* 1988)

Abstract—Transient boiling heat transfer characteristics of R113 at large stepwise power generation are investigated experimentally over a wide range of system pressures. The experimental results are summarized as follows. (1) There is a limiting value of heat flux, named transient critical heat flux, above which the effective heat removal in transient nucleate boiling cannot be expected. The transient critical heat flux becomes lower than the critical heat flux in the steady state under a low system pressure. (2) In the case of the low system pressure, the initial bubbles under the condition of near transient critical heat flux have the peculiar shape like a 'straw hat'. The boiling transition can be explained due to the consumption of the nucleate boiling liquid layer. In the case of high system pressure, however, no massive vapor bubble appears in transient nucleate boiling and boiling transition occurs due to filling of the fine initial bubbles on the heat transfer surface.

1. INTRODUCTION

IN A MODERN power generation plant and an electric device, the thermal power density and the heat flux become higher and higher in order to realize the high efficient performance and to make the volume compact. During an accident of such a plant and a device, the transient high heat load which is much higher than the stationary boiling critical heat flux of liquid coolant may be produced locally. The state of high heat load, however, may vanish due to the inherent self-controllability and the auxiliary control system. Usually, the boiling transition is accompanied with the generation of massive vapor bubbles near the heat transfer surface, and it is necessary, in order to increase the wall temperature suddenly, that the vapor bubble spreads over a certain area and covers the heat transfer surface for a certain time. Therefore, when the heat load is local and pulse-wise, it may be possible to remove the transient heat load without any damage due to boiling transition. The subjects to research and develop are considered to search a suitable cooling method delaying the occurrence of boiling transition and increasing the total heat removal until boiling transition.

Previous research concerning the transient boiling transition has been focused on the burnout phenomena which occur in the exponentially increasing process of the heat generation rate, because the research objectives are to make clear the transient boiling heat transfer at the reactivity accident of a nuclear reactor. The results of this research indicate that the transient burnout heat flux is higher than the stationary burnout heat flux and it increases with the heating rate [1–5], where 'transient burnout' expresses the burnout in the transient power input and 'stationary burnout' the burnout in the stationary power input, respectively. The transient burnout mechanism is also discussed in the literature [2, 5, 6]. The bubble behavior near the transient burnout condition is considered to be in the extrapolated situation of the stationary burnout, because the heating rate is not extremely high and there is almost no data concerning the basic characteristics of boiling under the transient condition.

In such an accident as the quenching of a superconducting magnet, however, the energy stored in electromagnetic form is released instantaneously as thermal energy. In this case, it is important to know whether the total released thermal energy can be removed without any damage to the device, rather than whether the instantaneous heat flux exceeds the transient burnout heat flux. When the heat load changes stepwise, the instantaneous heat flux can theoretically increase with the rise of the heating step, and therefore, it is not reasonable that the transient burnout heat flux is regarded as the criterion for the boiling heat transfer.

In this study, the transient boiling experiment was performed under the stepwise heating condition over a wide range of system pressures from atmospheric to near critical pressure, to examine the effects of the wide variety of physical properties on the transient boiling mechanism. R113 was selected as the test

NOMENCLATURE

B.I.	boiling incipience
B.O.	boiling transition
c_p	specific heat [J kg^{-1} K^{-1}]
J	nucleation rate [m^{-3}]
Ja	Jakob number
K^*	Boltzmann's constant [J K^{-1}]
L	latent heat [J kg^{-1}]
m	molecular mass [kg]
M	total vapor generation rate [kg s^{-1}]
m_1	vapor generation rate from the spherical surface [kg s^{-1}]
m_2	vapor generation rate from the surrounding vapor brim [kg s^{-1}]
m_w	vapor generation rate from the bottom of the spherical portion of a large bubble [kg s^{-1}]
N	molecular number density [m^{-3}]
n	nucleation site density [cm^{-2}]
P	system pressure [MPa]
P_{cr}	critical pressure [MPa]
P_g	generated pressure by boiling [kPa]
Q	heat generation rate [MW m^{-2}]
q_l	net heat flux transferred to the fluid [MW m^{-2}]
$[q_l]$	heat removal during transient boiling [kJ m^{-2}]
R	bubble radius [m]
R_A	radius of the spherical surface [m]
R_B	radius of the surrounding vapor brim [m]
R^*	gas constant [J kg^{-1} K^{-1}]
t	time [s]
t_1	time when the vapor brim spreads over the whole heater surface [s]
t_2	time when the wall superheat reaches the peak [s]
V	volumetric concentration of bubbles per unit liquid volume
V^*	bubble volume distribution function.

Greek symbols

α_{nc}	void fraction in the nucleate boiling liquid layer
δ_{nc}	thickness of the nucleate boiling liquid layer [m]
δ_{sh}	thickness of the superheated liquid layer at boiling incipience [m]
θ	temperature [°C]
$\Delta\theta_{sat}$	wall superheat [K]
$\Delta\theta_{sub}$	liquid subcooling [K]
κ	thermal diffusivity [m^2 s^{-1}]
λ	thermal conductivity [W m^{-1} K^{-1}]
ρ	density [kg m^{-3}]
σ	surface tension [N m^{-1}].

Subscripts

CHFst	critical heat flux in stationary boiling
CHFtr	critical heat flux in transient boiling
Cu	copper foil heater
homo	homogeneous nucleation
l	liquid
r	epoxy resin
v	vapor
w	heat transfer wall.

fluid. Bubble behavior during transient boiling was observed by the high speed movie, and the transient boiling mechanism at the extremely high heat load was discussed. The heat removal by boiling was investigated by using the models based on the boiling transition mechanism.

2. EXPERIMENTAL APPARATUS AND PROCEDURES

The experimental apparatus for transient boiling is shown in Fig. 1 together with the test section. The pressure vessel contains about 7 liter of test fluid (R113). The system pressure, P, and the liquid temperature, θ_l, can be set up to the desired values up to 3.3 MPa and 230°C, respectively, by using pressurized nitrogen gas and an immersion heater. The accuracies of setting these values are ± 0.01 MPa and ± 1°C. The dissolved gas in the liquid is purged enough by using the vacuum pump before each experiment.

The test heater is a copper foil 7 μm thick laminated on the epoxy resin plate. The effective heating area is 4 mm wide and 40 mm long and its pattern is drawn together with the resistance measuring terminals by the etching method, as shown in Fig. 1. The heater is fixed horizontally upward in 60 mm of the liquid in the pressure vessel. The heat to start the transient boiling is generated by supplying a stepwise d.c. electric current to the copper foil by using the control signal, the power controller and the power supply, and the heat generation rate per unit heat transfer surface area can be controlled up to 150 MW m^{-2}.

The time histories of heat generation rate, Q, and the temperature of the test heater, θ_w, can be calculated by using measured results of the heating current and the electric resistance of the 14 mm long section at the center of the copper foil, and then, the heat flux transferred to the test fluid can be also calculated by taking account of the heat capacity of the foil and the transient thermal conduction in the epoxy plate. Here, the thermal time response and the temperature drop in the heater can be regarded as less than 0.2 μs and 0.1°C, respectively [7].

The pressure fluctuation due to incipience of tran-

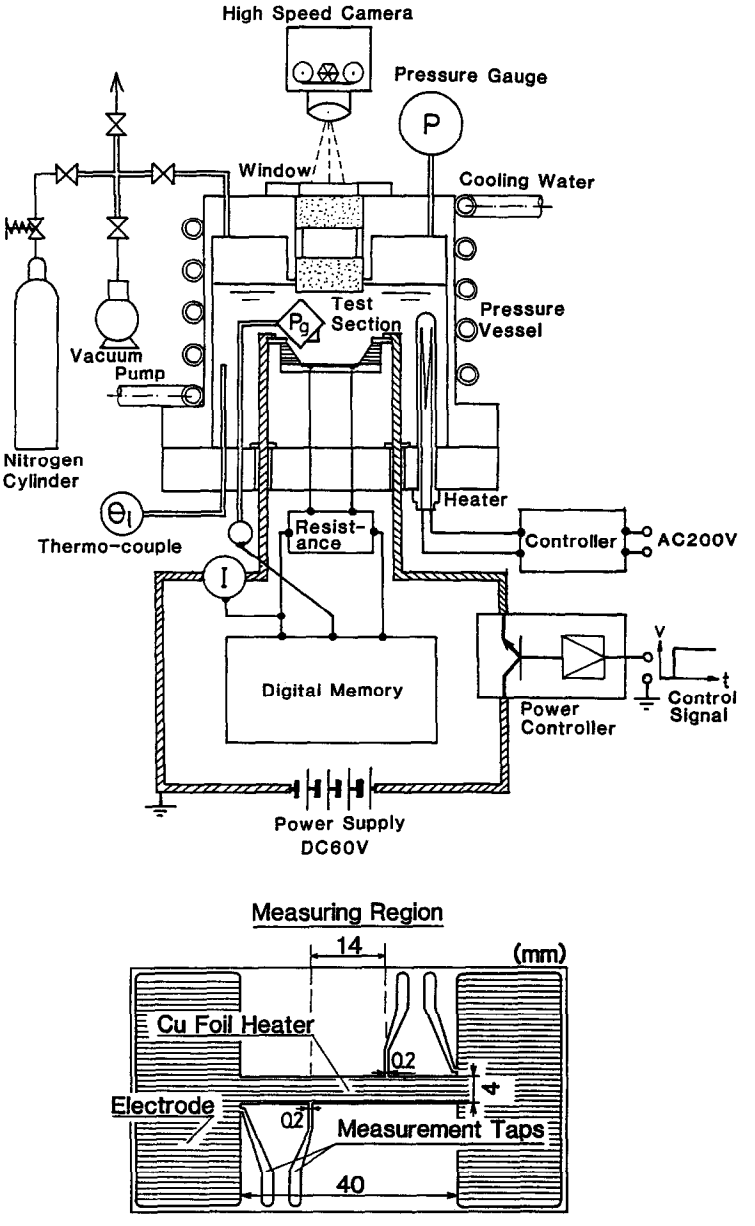

FIG. 1. Experimental apparatus for transient boiling.

sient boiling is measured by the semiconductor-type pressure transducer the eigenfrequency of which is 200 kHz and the sensitive surface is located 30 mm above the heater surface. The bubble behavior is observed by taking the high speed motion picture through the window of the pressure vessel. The detailed filming and lighting methods will be described in the following section.

3. EXPERIMENTAL RESULTS AND CONSIDERATIONS

3.1. *Transient boiling heat transfer at stepwise heat generation*

Figure 2 shows the measured and calculated time histories at the stepwise heat generation, where q_l, θ_w and P_g indicate the heat flux transferred to the fluid, wall temperature and generated pressure due to transient boiling, respectively. The time of boiling incipience (B.I.) is determined as that when the pressure fluctuation begins to occur. The time of boiling transition (B.O.) is judged from the rapid increase of θ_w and the rapid decrease of q_l. Since the thermal conductivity and the thermal diffusivity of R113 liquid are smaller than those of epoxy resin, the heat flux into the fluid is about 30% of the heat generation rate, Q, during transient heat conduction before boiling incipience and less than 50% of that even during boiling.

Figure 3 shows the changes of the wall superheat time history with the increase of stepwise heat generation rate, Q_0, in two cases of system pressure. At

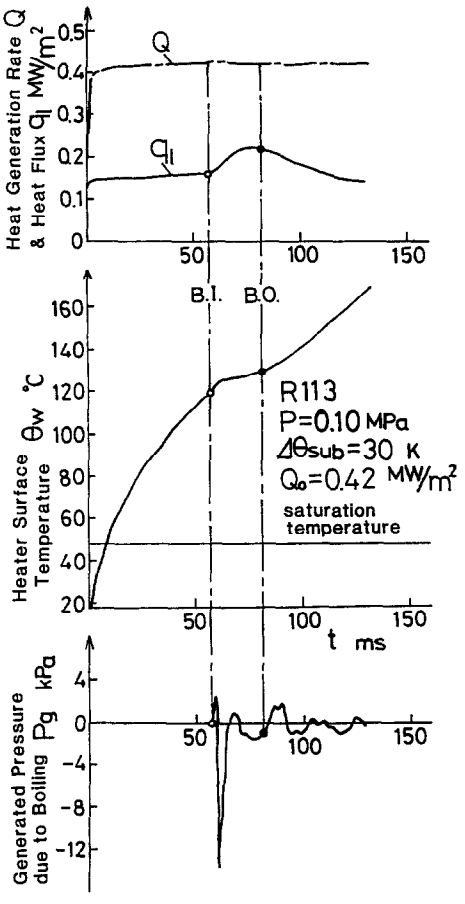

FIG. 2. Time histories of transient boiling heat transfer at stepwise heat generation.

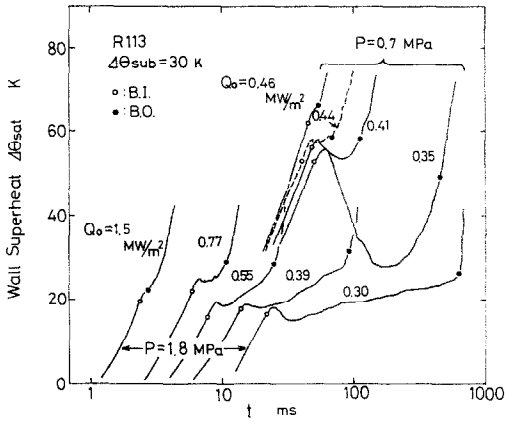

FIG. 3. Change of wall superheat time history with increase of stepwise heat generation.

the low heat generation rate, the wall superheat drops for a moment after boiling incipience, that is, a high heat flux exceeding the stepwise heat generation rate is instantaneously transferred to the fluid due to explosive boiling. However, as Q_0 is increased, the drop in wall superheat becomes hard to see, and simultaneously the duration of nucleate boiling becomes extremely short. At further slightly increased Q_0, the wall superheat goes on increasing even during nucleate boiling, that is, such a high heat load cannot be sufficiently removed by boiling heat transfer in spite of explosive boiling. From the observation of the bubble behavior described in the following section, such a rapid increase of wall superheat corresponds to the occurrence of boiling transition in the growing process of the initial bubbles on the heat transfer surface. It can be regarded as a criterion of the transient boiling heat transfer that whether the heat flux above the heat generation rate is transferred or not to the fluid during nucleate boiling. Therefore, when the stepwise heat generation rate is gradually increased, the heat flux at which the wall superheat at the inception of boiling persists during nucleate boiling can be defined as a 'transient boiling critical heat flux', q_{CHFtr}, which means the heat removal limit of transient boiling.

3.2. *Bubble behavior on transient critical heat flux conditions*

3.2.1. *High speed motion filming method.* The bubble behavior in transient boiling is not sufficiently known under such a high heat flux condition as the transient critical heat flux. In the following subsection, the bubble growth rate, the nucleation site density and the mechanism of the boiling transition in the transient boiling of R113 at the stepwise heat generation will be described, based on the observation by the high speed motion pictures.

As shown in Fig. 1, the high speed movie has been taken mainly looking down the heat transfer surface. In some cases, two mirrors as shown in Fig. 4 have been used, and both the top view and the side view of the bubble behavior have been filmed coincidently in order to get better understanding of the three-dimensional bubble behavior. The filming speed is between 5000 and 8000 f.p.s.

3.2.2. *Bubble behavior from boiling incipience to boiling transition.* Figures 5 and 6 show the typical results of high speed motion filming on the transient critical heat flux conditions in three cases of system pressure, where Fig. 5 shows the bubble behavior near boiling incipience and Fig. 6 that near boiling transition, respectively. In the 0.3 MPa case, the upper half in each frame of the photographs shows the side view of the bubble and the lower half shows the top view. At this pressure condition, an initial bubble grows in a peculiar shape accompanying the thin brim around a hemispherical shell. At boiling transition, there is a massive vapor bubble above the heat transfer surface. In the 0.7 MPa case, the thin vapor phase rapidly develops along the heat transfer surface, independently of the spherical bubbles growing on the edge of the heater. The heat transfer surface is still covered with the coalesced vapor bubble near boiling transition. In the 1.8 MPa case, many fine bubbles are produced simultaneously on the whole heat transfer surface at boiling incipience, and boiling transition occurs in the coalescing process of the initial bubbles.

Figure 7 illustrates a sketchy bubble behavior at

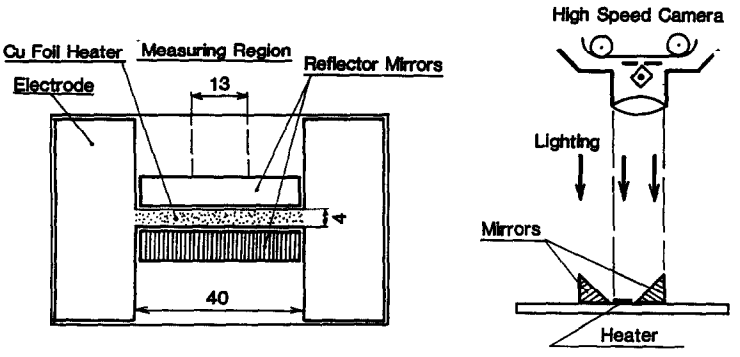

FIG. 4. High speed filming method.

these pressure conditions, based on the results of the high speed motion pictures, where the heat flux is nearly q_{CHFtr} at each pressure condition.

In the 0.3 MPa case, the initial bubble has the peculiar shape like a 'straw hat', the brim of which is made of a thin vapor film (<0.2 mm thick). The growing rate of the brim is faster than the hemispherical vapor shell. There is a time lag (about 3.5 ms) until the wall superheat history flattening after the heat transfer surface completely covered with the brim. In this duration, the residual liquid film beneath the brim, the thickness of which can be estimated to be about 10 μm, is transmitted to the nucleate boiling liquid layer, and then, nucleate boiling is made active. In the nucleate boiling liquid layer, the nucleation site density is nearly of the same order as the extrapolated value of the stationary boiling and the maximum bubble diameter is about 0.2 mm. The void fraction in the nucleate boiling liquid layer can be estimated to be less than 0.1, by using the measured nucleation site density and maximum bubble diameter. The nucleate boiling liquid layer, therefore, consists of almost only liquid, despite a large nucleation site density. Assuming that the wall heat load is removed by thermal conduction in the liquid part in the nucleate boiling liquid layer, the thickness of the liquid layer can be calculated as 16 μm. The growth of the hemispherical shell of the initial bubble is contributed by evaporation on the upper spherical shell and on the base of the hemisphere and by inflow vapor from the brim vapor film. The contribution of the base evaporation to the growth of the hemispherical shell is about 10%. The initial bubble grows, trapping the brim vapor film and the small bubbles in the nucleate boiling liquid layer, and finally, becomes spherical and departs from the heat transfer surface. After departure of the initial bubble, the plate-shaped coalesced bubble remains on the nucleate boiling liquid layer. Boiling transition occurs just after local vanishing of the nucleate boiling liquid layer during coalesced bubble growth.

In the 0.7 MPa case, the generation and the growth of the initial bubble are fairly different from those in the 0.3 MPa case. Initial spherical bubbles are generated on the edge of the heat transfer surface and their growth rate is fairly slow. Apart from the spherical bubbles, a thin vapor phase (<0.1 mm thick) develops rapidly in the shape of a cloud. This vapor phase may consist of many activated small bubbles, and cannot be recognized as a vapor film. Because the top view of the vapor phase does not exhibit a smooth curved line but a very complicated shape like a cloud, some part of the vapor phase edge is obscure. Moreover, since the wall temperature at boiling incipience is close to the homogeneous nucleation temperature, it may be possible to observe the bubble due to homogeneous nucleation. The characteristics of the nucleate boiling liquid layer produced after growth of the initial bubble and the mechanism of boiling transition are similar to those in the 0.3 MPa case.

In the 1.8 MPa case, no massive coalesced bubble is generated during the whole of the transient nucleate boiling. At boiling incipience, many fine bubbles generate simultaneously and uniformly on the heat transfer surface. The critical radius of nucleation can be estimated to be 0.01 μm, by using the measured wall superheat at boiling incipience. The heat transfer is enhanced just after boiling incipience since the time history of the wall superheat turns flat. Boiling transition occurs in the growing process of the initial bubbles due to filling of the bubbles on the heat transfer surface. Even at the occurrence of the boiling transition, the bubble diameter is considered to be of the order of 10 μm, based on the resolution of the high speed motion pictures.

3.2.3. *Growth rate of initial bubble in transient boiling.* In cases of $P < 0.5$ MPa, the initial bubble grows in the peculiar shape as shown in Fig. 7. From the wall temperature history, it is concluded that the heat transfer surface is not dry in spite of being almost covered with the vapor film, and there is a liquid film between the heat transfer surface and the vapor film. Both the growth of the spherical radius, R_B, and that of the brim, R_A, of the initial bubble are shown in Fig. 8, compared with the bubble growth of stationary boiling using Zuber's correlation [8] with the same wall superheat as the transient condition. Both R_A and R_B increase linearly with time, and the growth rates measured in this experiment are fairly faster than that of stationary boiling. The dependencies of the

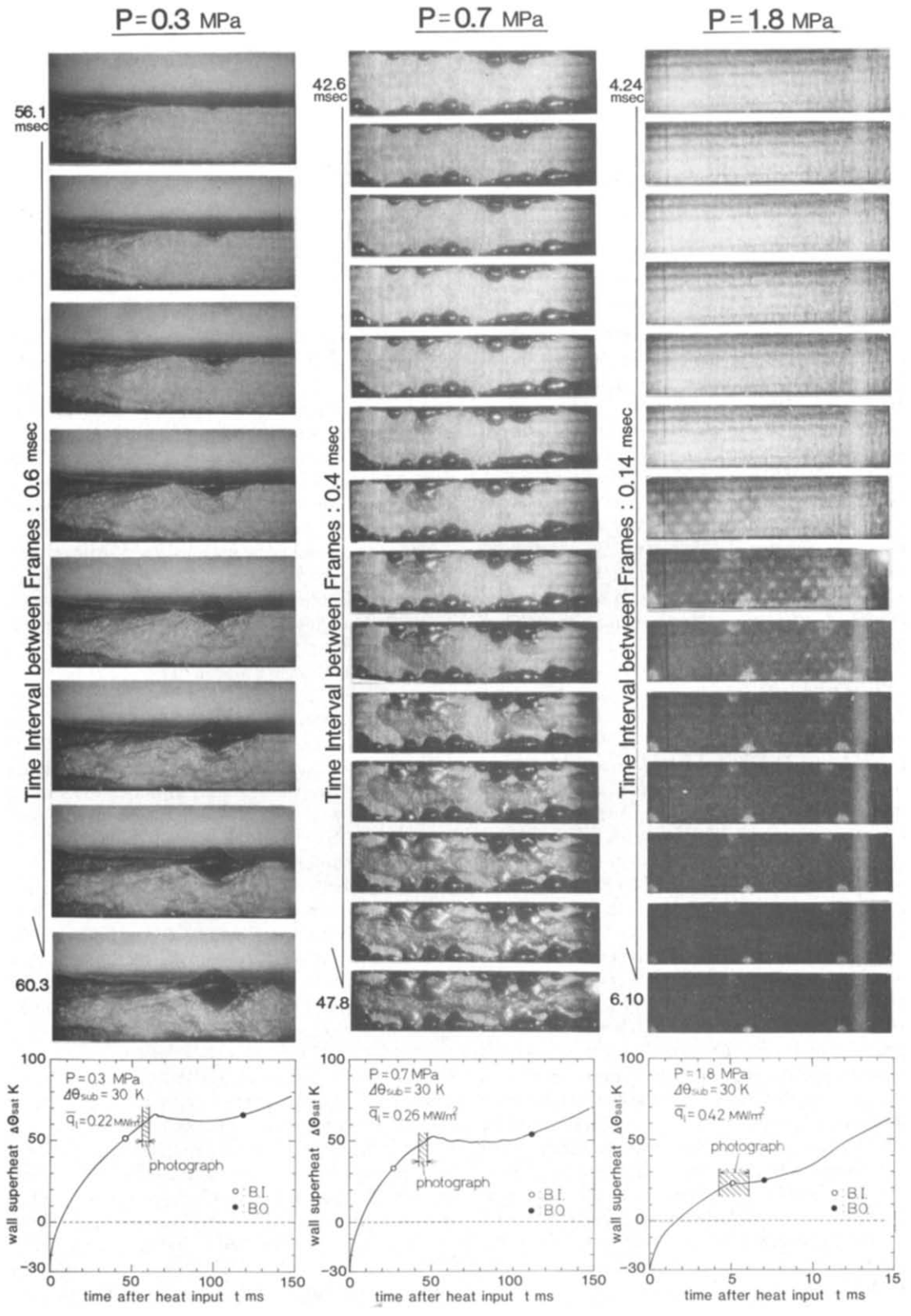

FIG. 5. Bubble behavior near boiling incipience.

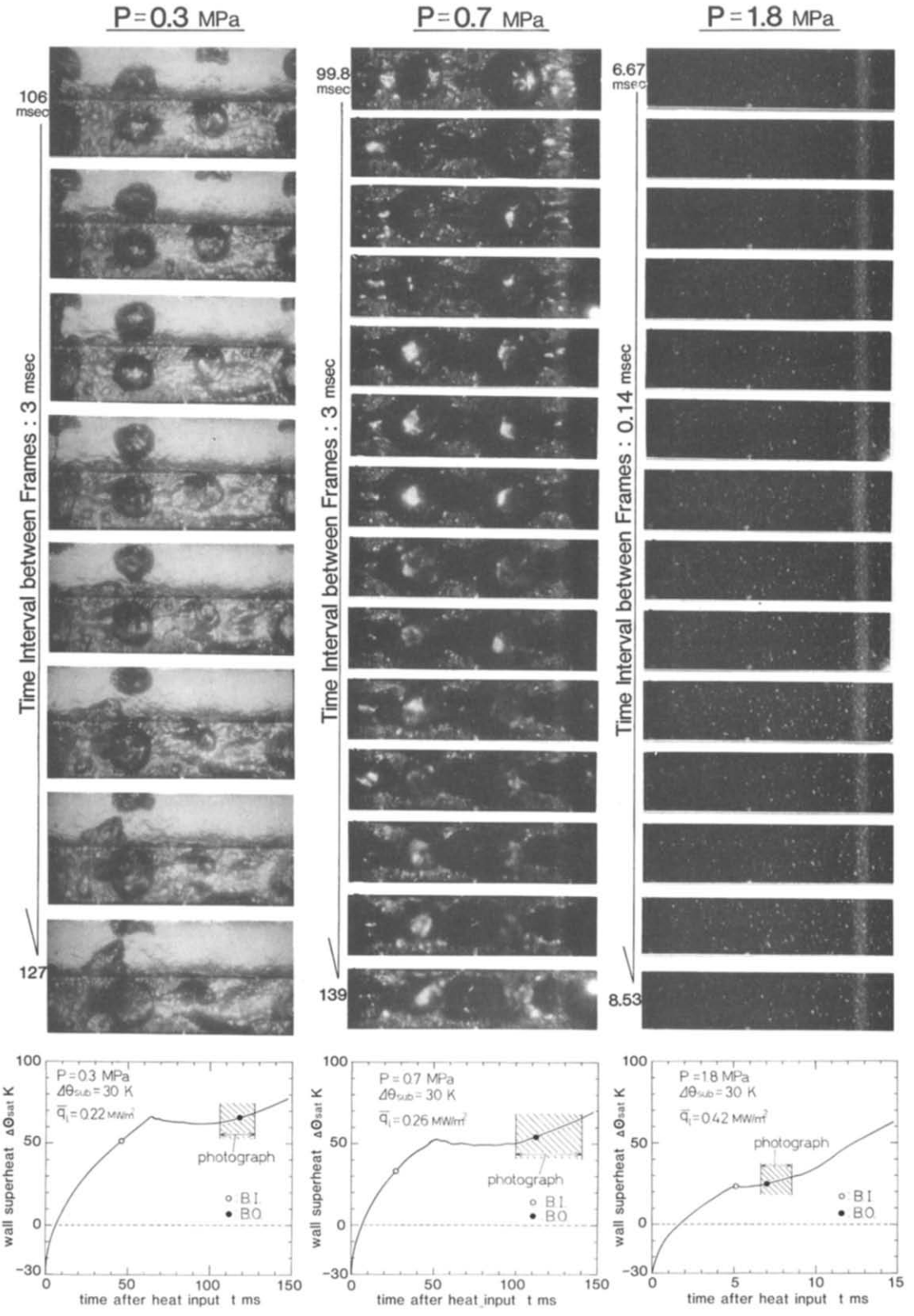

FIG. 6. Bubble behavior near boiling transition.

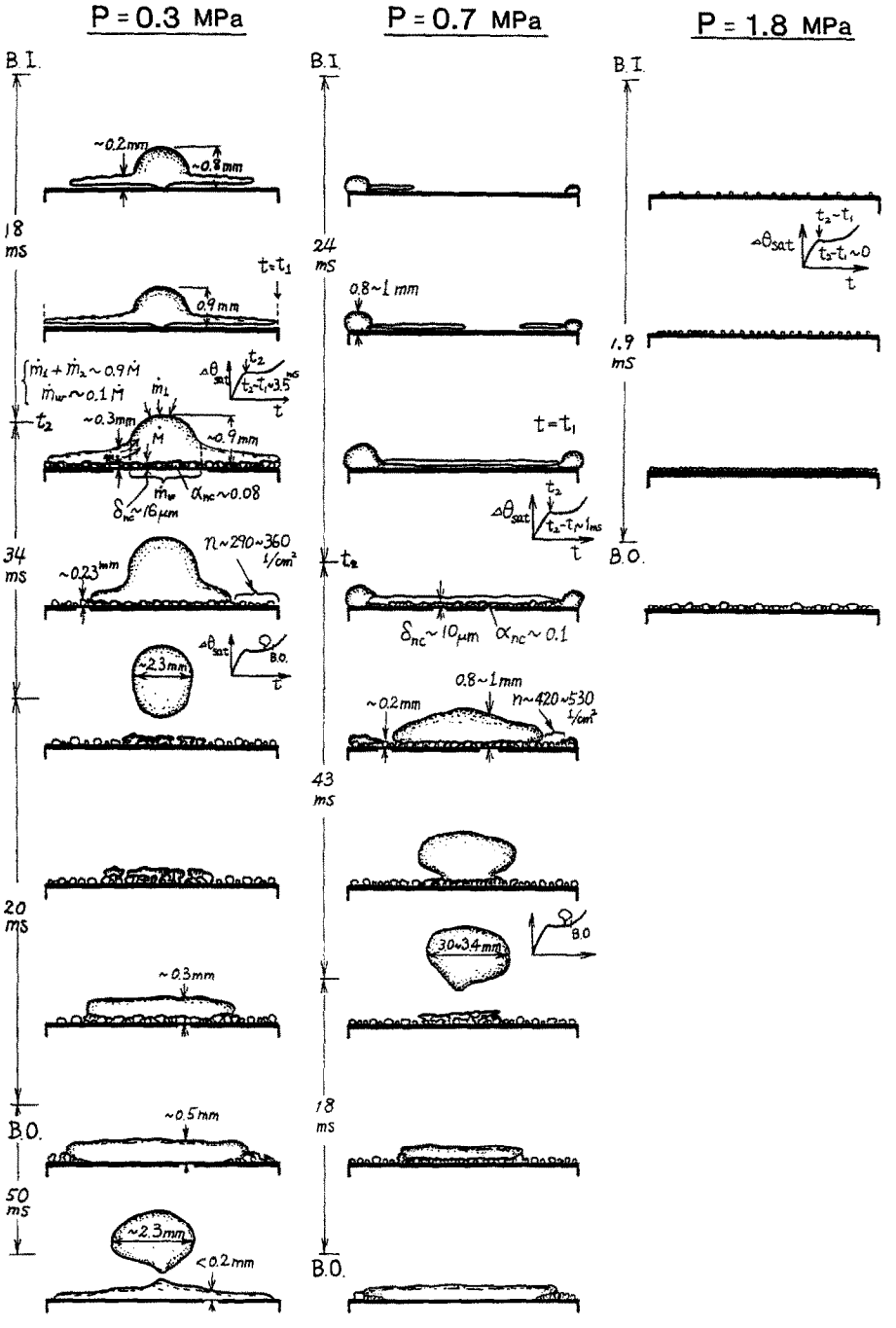

FIG. 7. Sketchy bubble behavior at transient heat generation.

growth rates on the system pressure, P, and on the Jakob number, Ja, are shown in Figs. 9(a) and (b), respectively, and the growth rates become slower with P and depend linearly on Ja. On the other hand, the bubble growth rate controlled by the inertia of the surrounding liquid can be approximately expressed as

$$\frac{dR}{dt} = \sqrt{\left(\frac{2}{3}\cdot\frac{P_v - P}{\rho_l}\right)} \qquad (1)$$

where the bubble pressure P_v is identified with the saturation pressure corresponding to the wall temperature at boiling incipience. The bubble growth rate predicted by this equation is about 16 m s^{-1}, independent of the system pressure, and considerably faster than the measured growth rates. The growth rate of the initial bubble, therefore, is still controlled by heat transfer, despite being extremely fast growing.

3.2.4. *Nucleation site density in transient boiling.*

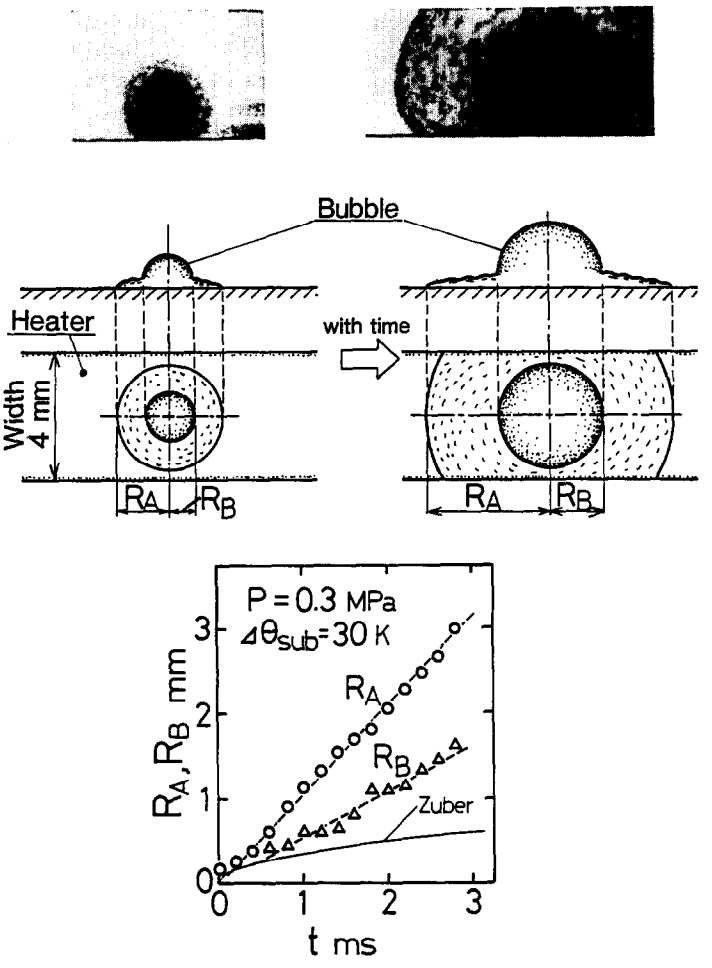

FIG. 8. Growth of 'straw hat' type bubble.

The nucleation site densities both of the initial bubble and in the nucleate boiling liquid layer are shown in Fig. 10. In this figure, Tien's correlation [9] for stationary boiling is compared. The nucleation site density of the initial bubble is very low and has strong dependency on the system pressure. On the other hand, the nucleation site density in the nucleate boiling liquid layer is very close to the extrapolation of the stationary boiling characteristics.

3.3. *Relation between transient critical heat flux and boiling transition mechanism*

From observation of the high speed movie, it has been recognized that the bubble behavior at the stepwise high heat generation is not only different from that of stationary boiling or that observed in the other studies on the transient boiling but also remarkably varies with the system pressure. Therefore, the transient critical heat flux defined in Section 3.1 may also vary correspondingly to the variety of the bubble behavior leading to boiling transition.

Figure 11 shows the dependency on the system pressure of the transient critical heat flux of R113, q_{CHFtr}, together with the stationary critical heat flux, q_{CHFst}, obtained in this experiment. As can be seen in the figure, the transient boiling heat removal attains a limiting value when the heat flux becomes about 60% of q_{CHFst} under the low pressure conditions, while q_{CHFtr} increases exceedingly under the medium pressure conditions where q_{CHFst} begins to decrease. After q_{CHFtr} exhibits the peak value, q_{CHFtr} has the same decreasing trend with increasing system pressure as that for q_{CHFst}. Under the high pressure condition (>1.5 MPa) q_{CHFtr} exceeds q_{CHFst}. The transient boiling heat removal near q_{CHFtr} conditions, which will be discussed in detail in the next section, is nearly 10 kJ m^{-2} and slightly increases with pressure, but the pressure dependency of the heat removal turns into a sharply decreasing trend at about 0.7 MPa and the heat removal on the high pressure condition becomes negligibly small.

A special feature of the transient boiling of R113 is that the wall superheat at the boiling incipience becomes extremely high under the low pressure conditions. The surface tension, σ, of R113 is very low compared with that of water and the wettability of the heat transfer surface with R113 liquid is very high, so that the nucleation cavity is apt to be filled with

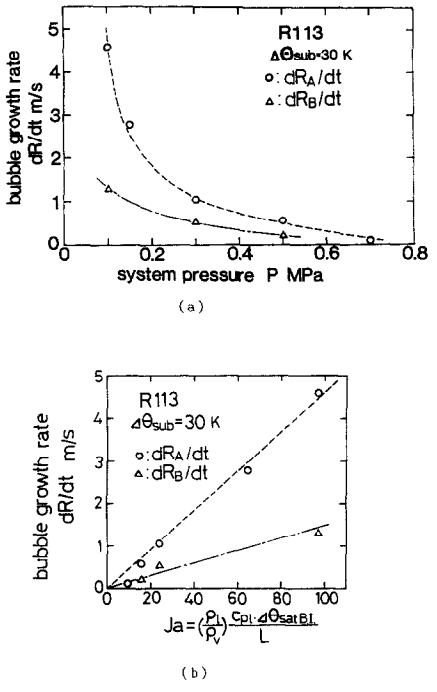

FIG. 9. Growth rate of initial bubble.

liquid and, in the result, few active cavities become active. Figure 12 shows the wall superheat at boiling incipience together with those under the conditions of the stationary critical heat flux and the homogeneous nucleation. As seen in the figure, the wall superheat of transient boiling is much higher than that of stationary boiling but lower than that of homogeneous nucleation under the low pressure conditions, and decreases with increasing the system pressure. From the comparison with Fig. 11, such three wall superheats become almost identical when the system pressure becomes 1.6 MPa where q_{CHFtr} indicates the peak value. The nucleation of transient boiling is considered to start still from cavities of the surface despite the extremely high wall superheat under the low pressure condition and to occur in nearly the same situation as the homogeneous nucleation under the high pressure condition.

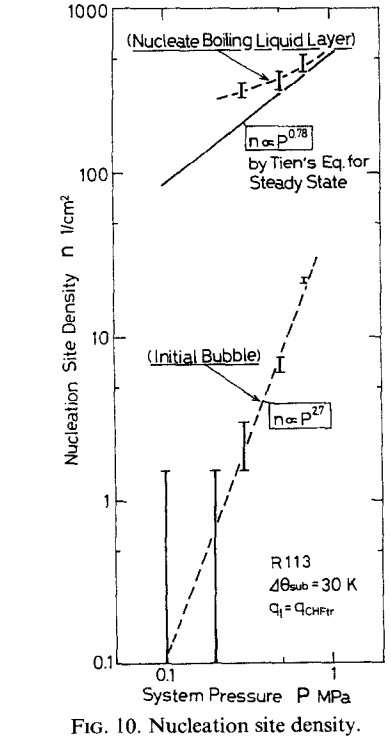

FIG. 10. Nucleation site density.

When the system pressure is less than 1.0 MPa, q_{CHFtr} is about 60% of q_{CHFst}. In the case of R113 under low pressure conditions, since the initial bubble growth is promoted due to energy release from the superheated liquid layer, the growth rate and size of the bubbles become much higher and larger than those of stationary boiling. The transient boiling transition, therefore, is apt to occur at lower heat flux than q_{CHFst}. On the other hand, the initial bubbles are very fine and are generated coherently on the heat transfer surface under the high pressure condition. Boiling heat transfer, therefore, becomes very high just after boiling incipience, but boiling transition occurs immediately after the heat transfer surface is filled with the fine bubbles, so that transient boiling heat removal is very small.

3.4. *Relation between transient critical heat flux and boiling heat removal*

From the observation of the high speed movie, it has been confirmed that even under transient critical heat flux conditions, there exists the nucleate boiling liquid layer similar to that of stationary boiling in the low pressure range. Moreover, it is unquestionable that the transient boiling heat transfer is not effective until formation of the nucleate boiling liquid layer and that the consumption of the liquid layer corresponds to the occurrence of the boiling transition.

Assuming that the thickness of the transient nucleate boiling liquid layer is expressed as Haramura and Katto's correlation [10], the transient boiling heat removal becomes

$$[q_l] = \rho_l L \delta_{nc} = 0.00536(\rho_l L) \times \frac{\sigma \rho_v}{(q_l/L)^2}\left(\frac{\rho_v}{\rho_l}\right)^{0.4}\left(1+\frac{\rho_v}{\rho_l}\right). \quad (2)$$

In Fig. 13, the experimental data of $[q_l]$ are compared with equation (2), where $q_l = q_{CHFtr}$. The agreement between them is quite good, considering the scattering of the experimental data. For $P = 1.8$ MPa, the difference between them is large, since the bubble behavior on this pressure condition is quite different from that at other pressure conditions as shown in Fig. 7 and the occurrence of boiling transition does not relate to the nucleate boiling liquid layer.

From the observation of the bubble behavior, at a higher heat flux condition than q_{CHFtr}, there is no period when the heat is transferred through the

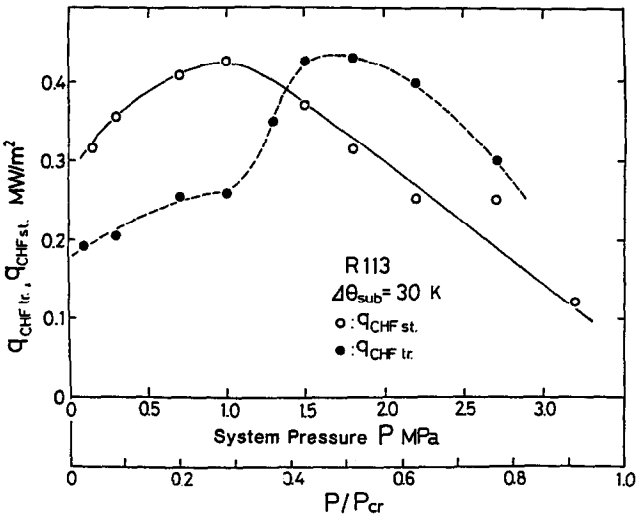

FIG. 11. Transient critical heat flux.

nucleate boiling liquid layer and the rapid increase of the wall temperature corresponding to the boiling transition is observed in the growing process of the initial bubbles. The distance from the heat transfer surface to the vapor film or phase as shown in Fig. 5 is considered to be less than the thickness of the superheated liquid layer formed until boiling incipience δ_{sh}, because the growth of these vapor parts is contributed to by the energy supply from this liquid layer, too. The heat removal up to complete evaporation of this liquid layer is

$$[q_l] = \rho_l L \delta_{sh}. \tag{3}$$

Using liquid thermal conductivity, λ_l, and the wall superheat at boiling incipience, $\Delta\theta_{satB.I.}$, δ_{sh} is

$$\delta_{sh} = \lambda_l \Delta\theta_{satB.I.}/q_l. \tag{4}$$

From equations (3) and (4)

$$[q_l] = \rho_l L \lambda_l \Delta\theta_{satB.I.}/q_l. \tag{5}$$

In Fig. 13, equation (5), where $q_l = q_{CHFtr}$, is shown by the dotted line. The heat removal calculated by equation (5) is less than one half of that calculated by equation (2). This result corresponds to the remarkable decrease of the heat removal for $q_l > q_{CHFtr}$.

3.5. *Examination based on homogeneous nucleation theory*

As described in the preceding section, under the high pressure condition of $P > 1.6$ MPa, the wall tem-

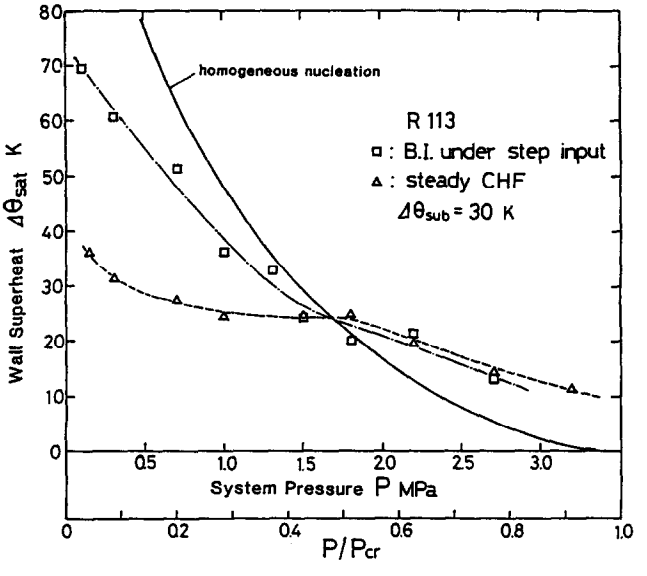

FIG. 12. Comparison among wall superheats.

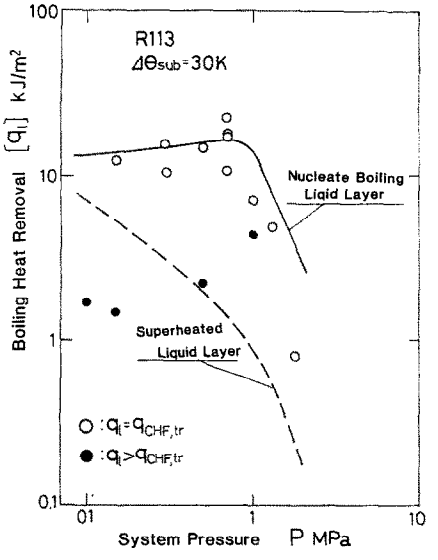

FIG. 13. Transient boiling heat removal.

perature at boiling incipience on the transient critical heat flux condition becomes nearly equal to the homogeneous nucleation temperature, and then, numerous fine initial bubbles are produced instantaneously on the whole heat transfer surface. With the stepwise high heating, therefore, nucleation may occur preferentially in a homogeneous rather than a heterogeneous manner under such a high pressure condition. Moreover, the boiling transition occurs just after the repletion of the initial bubbles. In this section, several characteristic quantities based on homogeneous nucleation theory are calculated and discussed in comparison with the experimental results.

The nucleation rate J (nuclei m^{-3}) in a liquid at a system pressure, P, and temperature, θ, based on homogeneous nucleation theory is given by

$$J = N\left(\frac{6\sigma}{\pi m}\right)^{0.5} \exp\left(-\frac{L}{R^*\theta}\right) \times \exp\left(-\frac{16\pi\sigma^3}{3K^*\theta(P_v-P)^2}\right) \quad (6)$$

where the vapor pressure, P_v, is related to θ by using the following equation derived from the Clapeyron–Clausius equation:

$$P_v - P = P\left[\exp\left(\frac{L}{R^*}\cdot\frac{\Delta\theta_{sat}}{\theta\cdot\theta_{sat}}\right) - 1\right]. \quad (7)$$

It can be seen from equations (6) and (7) that the nucleation rate tremendously increases with slightly increasing θ near the homogeneous nucleation temperature. On the other hand, the bubble growth is controlled by the inertia of the surrounding liquid in the early stage and controlled by the heat flow from the superheated liquid to the vapor–liquid interface in the following stage. In each stage, the bubble growth can be expressed, respectively, as follows:

$$R = \sqrt{\left(\frac{2}{3}\cdot\frac{P_v-P}{\rho_l}\right)t} \quad (8)$$

$$R = \sqrt{(\pi\kappa_l)}\frac{\rho_l}{\rho_v}\cdot\frac{c_{pl}\Delta\theta_{sat}}{L}t^{0.5}. \quad (9)$$

Based on the nucleation rate corresponding to the wall temperature, θ_w, and the bubble growth, the volumetric fraction of bubbles per unit liquid volume, V, can be expressed as

$$V(t) = \int_0^t \frac{dJ}{d\tau}\cdot\frac{4}{3}\pi[R(t-\tau)]^3\,d\tau \quad (10)$$

where $dJ/d\tau = dJ/d\theta_w \cdot d\theta_w/d\tau$, and $d\theta_w/d\tau$ is determined with the solution of the transient heat conduction equation at the stepwise heat generation in a semi-infinite medium

$$\frac{d\theta_w}{dt_l} = B\cdot\exp(A^2 t_l)\cdot\mathrm{erfc}(A\sqrt{t_l}) \quad (11)$$

where t_l expresses the time after the stepwise heating starts, and

$$A = \frac{\lambda_r/\sqrt{\kappa_r}+\lambda_l/\sqrt{\kappa_l}}{(c_p\rho\delta)_{Cu}}, \quad B = \frac{Q_0}{(c_p\rho\delta)_{Cu}}. \quad (12)$$

Figure 14 shows the calculated results of the time histories of J, θ_w and V in three cases of high system pressure of $P > 1.0$ MPa, where the heat generation rate is identical with the experimental result at which the transient critical heat flux is obtained. It will be seen in the figure that V rapidly increases in the short period of an order of 0.1 ms and immediately reaches 1, that is, the bubbles replete. Such a sudden increase of V depends on the explosive nucleation and the rapid growth of bubbles. The wall temperature rises only about 0.5 K in the duration from the incipience

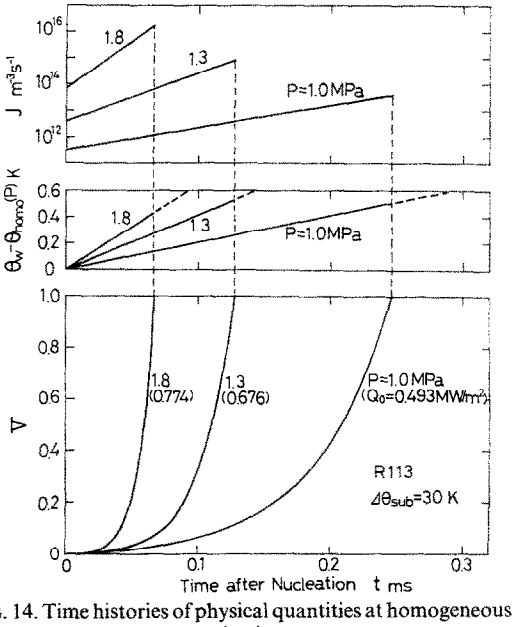

FIG. 14. Time histories of physical quantities at homogeneous nucleation.

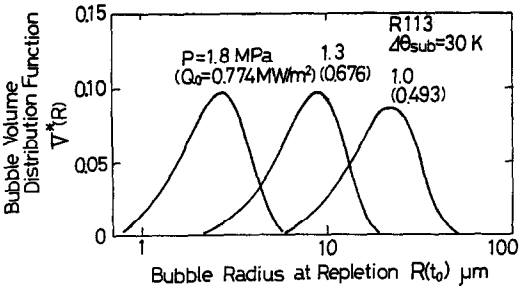

FIG. 15. Bubble volume spectra at repletion.

of bubble nucleation to bubble repletion, but the nucleation rate increases by about 200 times with such a little rise of wall temperature. The size of present bubbles can be expressed as the bubble volume spectrum. Figure 15 gives the volume distribution function $V^*(R)$, which is defined so that $V^*(R)\,dR$ is the total volume of all bubbles within the size range R to $R+dR$, where the spectra show those at the time when the bubbles replete. Taking the radius corresponding to the median of each distribution, the bubble size is less than 20 μm even in the case of a lower system pressure, 1.0 MPa. These features of the physical quantities as predicted in Figs. 14 and 15 are qualitatively identical with the trends of the experimental results in the case of the high pressure condition as shown in Fig. 5 ($P = 1.8$ MPa). The time until bubble repletion, however, is much shorter than the experimental result, because the wall temperature rise rate is suppressed due to the good heat transfer subsequent to explosive boiling, therefore, the nucleation rate may be less than that predicted with the pure homogeneous nucleation theory. Moreover, the thickness of the superheated liquid layer in which homogeneous nucleation may occur is estimated to be about 0.1 μm, therefore, a significant proportion of bubbles will penetrate through such a thin layer by repletion. For a further exact description of the boiling process under the high pressure condition, it is necessary to take account of the suppression effects of the heat transfer from the wall on the nucleation and the temperature distribution in the superheated liquid.

4. CONCLUSIONS

(1) There is a limiting value of heat flux, named transient critical heat flux, above which the heat flux cannot exceed the heat generation rate during transient nucleate boiling and also the heat in this duration can hardly be removed. The transient critical heat flux becomes lower than the critical heat flux in steady state under low system pressure, because the superheat energy stored in the thermal liquid layer at the boiling incipience becomes remarkably high.

(2) In the case of the low system pressure, since R113 has a high wettability with the heat transfer surface, the initial bubbles under the condition of near transient critical heat flux grow in the peculiar shape like a 'straw hat'. The boiling transition can be explained due to the consumption of the nucleate boiling liquid layer.

(3) In the case of the high system pressure, no massive vapor bubble appears in the transient nucleate boiling and the boiling transition occurs due to filling of the fine initial bubbles on the heat transfer surface. The feature of boiling nucleation can be explained to some extent by homogeneous nucleation theory.

REFERENCES

1. H. A. Johnson, Transient boiling heat transfer to water, *Int. J. Heat Mass Transfer* **14**, 67–82 (1971).
2. H. Kawamura, F. Tachibana and M. Akiyama, Heat transfer and DNB heat flux in transient boiling, *Proc. 4th Int. Heat Transfer Conf.*, No. B3.3 (1970).
3. A. Sakurai and M. Shiotsu, Transient pool boiling heat transfer (II), *J. Heat Transfer* **99**, 554–560 (1977).
4. I. Kataoka, A. Serizawa and A. Sakurai, Transient boiling heat transfer under forced convection, *Int. J. Heat Mass Transfer* **26**, 583–595 (1983).
5. S. Aoki, Y. Kozawa and H. Iwasaki, Boiling and burnout phenomena under transient heat input, *Trans. J.S.M.E.* **41**, 2950–2959 (1975) (in Japanese).
6. A. Serizawa, Theoretical prediction of maximum heat flux in power transients, *Int. J. Heat Mass Transfer* **26**, 921–932 (1983).
7. Y. Kozawa, S. Aoki, A. Inoue and K. Okuyama, Transient boiling heat transfer in a narrow channel (1st Report, Transient boiling characteristics under stepwise heat input), *Trans. J.S.M.E.* **48**, 2547–2555 (1982) (in Japanese).
8. N. Zuber, Hydrodynamic aspects of boiling heat transfer, AEC Report No. AECU-4439 (1959).
9. C. L. Tien, A hydrodynamic model for nucleate pool boiling, *Int. J. Heat Mass Transfer* **5**, 533–540 (1962).
10. Y. Haramura and Y. Katto, A new hydrodynamic model of critical heat flux, applicable widely to both pool and forced convection boiling on submerged bodies in saturated liquids, *Int. J. Heat Mass Transfer* **26**, 389–399 (1983).

CARACTERISTIQUES DU TRANSFERT THERMIQUE AVEC EBULLITION VARIABLE POUR DU R113 ET DES GRANDS ECHELONS DE PUISSANCE DE CHAUFFAGE

Résumé—Les caractéristiques du transfert thermique avec ébullition variable pour du R113 et des grands échelons de puissance sont étudiés expérimentalement dans un large domaine de pression. Les résultats expérimentaux sont les suivants: (1) il y a une valeur limite du flux de chaleur, appelée flux thermique critique transitoire, au dessus duquel l'enlèvement de chaleur par ébullition nucléée transitoire ne peut être espéré et le flux critique transitoire devient plus faible que le flux critique de régime permanent à faible pression; (2) dans le cas de faible pression, les bulles initiales, sous la condition proche du flux critique transitoire ont une forme particulière de "chapeau de paille". La transition d'ébullition peut être expliquée par la consommation de la couche liquide d'ébullition nucléée. Dans le cas des fortes pressions, il n'apparait pas de bulles de vapeur massives dans l'ébullition nucléée variable et la transition est due au remplissage des petites bulles initiales sur la surface chauffante.

DAS WÄRMEÜBERGANGSVERHALTEN BEI INSTATIONÄREM SIEDEN VON R113 BEI GROSSER STUFENWEISER WÄRMEZUFUHR

Zusammenfassung—Das Wärmeübergangsverhalten bei instationärem Sieden von R113 bei großer stufenweiser Wärmezufuhr wird experimentell über einen weiten Bereich des Systemdrucks untersucht. Die experimentellen Ergebnisse werden wie folgt zusammengefaßt: (1) Es existiert ein Grenzwert für die Wärmestromdichte, genannt instationäre kritische Wärmestromdichte, oberhalb der eine effektive Wärmeabfuhr bei instationärem Blasensieden nicht erwartet werden kann. Die instationäre kritische Wärmestromdichte wird bei kleinen Systemdrücken kleiner als die kritische Wärmestromdichte im stationären Zustand. (2) Im Fall des niedrigen Systemdrucks haben die ersten entstehenden Blasen unter Bedingungen nahe der instationären kritischen Wärmestromdichte eine eigenartige Form wie ein "Strohhut". Der Übergang zwischen den Siedebereichen kann durch den Abbau des Flüssigkeitsfilms beim Blasensieden erklärt werden. Bei hohen Systemdrücken tritt bei instationärem Blasensieden jedoch keine große Dampfblase auf. Der Übergang zwischen den Siedebereichen wird dadurch verursacht, daß die feinen ersten Blasen die Wärmeübertragungsfläche bedecken.

ХАРАКТЕРИСТИКИ ТЕПЛОПЕРЕНОСА ПРИ ПЕРЕХОДНОМ КИПЕНИИ ФРЕОНА 113 В СЛУЧАЕ СТУПЕНЧАТЫХ ЭНЕРГОВЫДЕЛЕНИЙ БОЛЬШОЙ МОЩНОСТИ

Аннотация—Экспериментально исследуются характеристики теплопереноса при переходном кипении фреона 113 в случае ступенчатых энерговыделений большой мощности в широком диапазоне давлений. Данные экспериментов обобщаются следующим образом: (1) Существует предельная величина теплового потока, названная переходным критическим тепловым потоком, выше которой нельзя ожидать эффективного отвода тепла при переходном пузырьковом кипении. При низком давлении в системе переходный критический тепловой поток становится меньше стационарного; (2) При низком давлении в системе зарождающиеся пузырьки в условиях, близких к переходному критическому тепловому потоку, имеют специфическую форму "соломенной шляпы". Режим переходного кипения можно объяснить поглощением образующегося слоя кипящей жидкости. В случае высокого давления пузырьки пара заполняют не объемный массив, а поверхность теплопереноса.